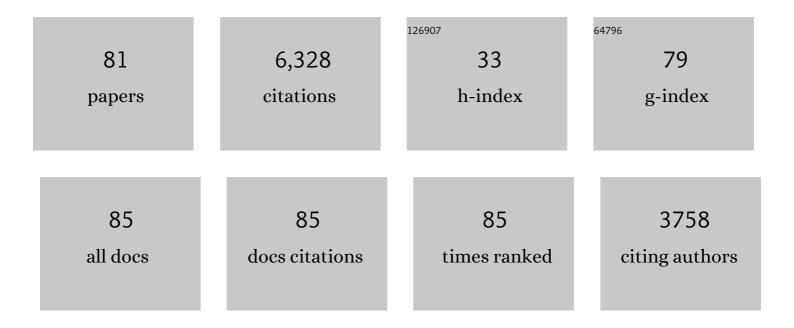
## Donald W Brown

List of Publications by Year in descending order

Source: https://exaly.com/author-pdf/9367313/publications.pdf Version: 2024-02-01



#	Article	IF	CITATIONS
1	Enhanced ductility in strongly textured magnesium produced by equal channel angular processing. Scripta Materialia, 2004, 50, 377-381.	5.2	546
2	Study of slip mechanisms in a magnesium alloy by neutron diffraction and modeling. Scripta Materialia, 2003, 48, 1003-1008.	5.2	529
3	An Experimental Investigation into Additive Manufacturing-Induced Residual Stresses in 316L Stainless Steel. Metallurgical and Materials Transactions A: Physical Metallurgy and Materials Science, 2014, 45, 6260-6270.	2.2	473
4	Twinning–detwinning behavior during the strain-controlled low-cycle fatigue testing of a wrought magnesium alloy, ZK60A. Acta Materialia, 2008, 56, 688-695.	7.9	453
5	Reorientation and stress relaxation due to twinning: Modeling and experimental characterization for Mg. Acta Materialia, 2008, 56, 2456-2468.	7.9	415
6	Internal strain and texture evolution during deformation twinning in magnesium. Materials Science & Engineering A: Structural Materials: Properties, Microstructure and Processing, 2005, 399, 1-12.	5.6	390
7	Validating a polycrystal model for the elastoplastic response of magnesium alloy AZ31 using in situ neutron diffraction. Acta Materialia, 2006, 54, 4841-4852.	7.9	390
8	Grain size effects on the tensile properties and deformation mechanisms of a magnesium alloy, AZ31B, sheet. Materials Science & Engineering A: Structural Materials: Properties, Microstructure and Processing, 2008, 486, 545-555.	5.6	359
9	Internal stress relaxation and load redistribution during the twinning–detwinning-dominated cyclic deformation of a wrought magnesium alloy, ZK60A. Acta Materialia, 2008, 56, 3699-3707.	7.9	261
10	The effects of texture and extension twinning on the low-cycle fatigue behavior of a rolled magnesium alloy, AZ31B. Materials Science & Engineering A: Structural Materials: Properties, Microstructure and Processing, 2010, 527, 7057-7067.	5.6	170
11	A polycrystal plasticity model for predicting mechanical response and texture evolution during strain-path changes: Application to beryllium. International Journal of Plasticity, 2013, 49, 185-198.	8.8	141
12	Role of twinning in the hardening response of zirconium during temperature reloads. Acta Materialia, 2006, 54, 2887-2896.	7.9	140
13	Role of twinning and slip during compressive deformation of beryllium as a function of strain rate. International Journal of Plasticity, 2012, 29, 120-135.	8.8	105
14	Micromechanical quantification of elastic, twinning, and slip strain partitioning exhibited by polycrystalline, monoclinic nickel–titanium during large uniaxial deformations measured via in-situ neutron diffraction. Journal of the Mechanics and Physics of Solids, 2013, 61, 2302-2330.	4.8	105
15	Structural representation of additively manufactured 316L austenitic stainless steel. International Journal of Plasticity, 2019, 118, 70-86.	8.8	99
16	Evaluation of a thermomechanical model for prediction of residual stress during laser powder bed fusion of Ti-6Al-4V. Additive Manufacturing, 2019, 27, 489-502.	3.0	93
17	Tailored thermal expansion alloys. Acta Materialia, 2016, 102, 333-341.	7.9	92
18	Influence of the Tool Pin and Shoulder on Microstructure and Natural Aging Kinetics in a Friction-Stir-Processed 6061–T6 Aluminum Alloy. Metallurgical and Materials Transactions A: Physical Metallurgy and Materials Science, 2007, 38, 69-76.	2.2	80

#	Article	IF	CITATIONS
19	Neutron diffraction measurements of residual stress in additively manufactured stainless steel. Materials Science & Engineering A: Structural Materials: Properties, Microstructure and Processing, 2016, 678, 291-298.	5.6	78
20	The influence of interstitial oxygen and peak pressure on the shock loading behavior of zirconium. Acta Materialia, 2005, 53, 1751-1758.	7.9	77
21	Coupled experimental and computational study of residual stresses in additively manufactured Ti-6Al-4V components. Materials Letters, 2018, 231, 221-224.	2.6	69
22	Directional and oscillating residual stress on the mesoscale in additively manufactured Ti-6Al-4V. Acta Materialia, 2019, 168, 299-308.	7.9	62
23	Critical comparison of two independent measurements of residual stress in an electron-beam welded uranium cylinder: Neutron diffraction and the contour method. Acta Materialia, 2011, 59, 864-873.	7.9	58
24	Dislocation structure evolution induced by irradiation and plastic deformation in the Zr–2.5Nb nuclear structural material determined by neutron diffraction line profile analysis. Acta Materialia, 2012, 60, 5567-5577.	7.9	56
25	Young's modulus evolution and texture-based elastic–inelastic strain partitioning during large uniaxial deformations of monoclinic nickel–titanium. Acta Materialia, 2013, 61, 1944-1956.	7.9	54
26	An analysis of phase stresses in additively manufactured 304L stainless steel using neutron diffraction measurements and crystal plasticity finite element simulations. International Journal of Plasticity, 2019, 121, 201-217.	8.8	51
27	Elastic Residual Strain and Stress Measurements and Corresponding Part Deflections of 3D Additive Manufacturing Builds of IN625 AM-Bench Artifacts Using Neutron Diffraction, Synchrotron X-Ray Diffraction, and Contour Method. Integrating Materials and Manufacturing Innovation, 2019, 8, 318-334.	2.6	45
28	Temperature and direction dependence of internal strain and texture evolution during deformation of uranium. Materials Science & amp; Engineering A: Structural Materials: Properties, Microstructure and Processing, 2009, 512, 67-75.	5.6	39
29	The influence of phase and substructural evolution during dynamic loading on subsequent mechanical properties of zirconium. Acta Materialia, 2013, 61, 7712-7719.	7.9	38
30	Neutron diffraction study of the deformation mechanisms of the uranium–7wt.% niobium shape memory alloy. Materials Science & Engineering A: Structural Materials: Properties, Microstructure and Processing, 2006, 421, 15-21.	5.6	37
31	Deformation behavior of additively manufactured GP1 stainless steel. Materials Science & Engineering A: Structural Materials: Properties, Microstructure and Processing, 2017, 696, 331-340.	5.6	37
32	Low temperature age hardening in U–13at.% Nb: An assessment of chemical redistribution mechanisms. Journal of Nuclear Materials, 2009, 393, 282-291.	2.7	36
33	Signatures of the unique microstructure of additively manufactured steel observed via diffraction. Scripta Materialia, 2018, 155, 16-20.	5.2	34
34	Predicting deformation behavior of α-uranium during tension, compression, load reversal, rolling, and sheet forming using elasto-plastic, multi-level crystal plasticity coupled with finite elements. Journal of the Mechanics and Physics of Solids, 2020, 138, 103924.	4.8	34
35	Influence of strain rate on mechanical properties and deformation texture of hot-pressed and rolled beryllium. Materials Science & Engineering A: Structural Materials: Properties, Microstructure and Processing, 2010, 527, 5181-5188.	5.6	32
36	Stability of the two-phase (α/ω) microstructure of shocked zirconium. Acta Materialia, 2014, 67, 383-394.	7.9	31

#	Article	IF	CITATIONS
37	Effects of heat treatment and build orientation on the evolution of Ϊμ and α′ martensite and strength during compressive loading of additively manufactured 304L stainless steel. Acta Materialia, 2020, 195, 59-70.	7.9	29
38	The Role of Texture, Temperature and Strain Rate in the Activity of Deformation Twinning. Materials Science Forum, 2005, 495-497, 1037-1042.	0.3	28
39	Twinning and de-twinning in beryllium during strain path changes. Materials Science & Engineering A: Structural Materials: Properties, Microstructure and Processing, 2013, 559, 29-39.	5.6	26
40	Tailoring Microstructure and Mechanical Properties of Additively-Manufactured Ti6Al4V Using Post Processing. Materials, 2021, 14, 658.	2.9	26
41	Effect of the scanning strategy on the formation of residual stresses in additively manufactured Ti-6Al-4V. Additive Manufacturing, 2021, 45, 102003.	3.0	26
42	Development of intergranular thermal residual stresses in beryllium during cooling from processing temperatures. Acta Materialia, 2009, 57, 972-979.	7.9	24
43	The effect of low-temperature aging on the microstructure and deformation of uranium- 6Âwt% niobium: An in-situ neutron diffraction study. Journal of Nuclear Materials, 2016, 481, 164-175.	2.7	23
44	Neutron and X-ray diffraction analysis of the effect of irradiation dose and temperature on microstructure of irradiated HT-9 steel. Journal of Nuclear Materials, 2013, 443, 522-530.	2.7	22
45	High Pressure Phase-Transformation Induced Texture Evolution and Strengthening in Zirconium Metal: Experiment and Modeling. Scientific Reports, 2015, 5, 12552.	3.3	21
46	Neutron and X-ray diffraction studies and cohesive interface model of the fatigue crack deformation behavior. Philosophical Magazine Letters, 2008, 88, 553-565.	1.2	20
47	A study of twinning in zirconium using neutron diffraction and polycrystalline modeling. Metallurgical and Materials Transactions A: Physical Metallurgy and Materials Science, 2002, 33, 757-763.	2.2	20
48	A study of twinning in zirconium using neutron diffraction and polycrystalline modeling. Metallurgical and Materials Transactions A: Physical Metallurgy and Materials Science, 2002, 33, 757-763.	2.2	19
49	In-situ high-energy X-ray diffraction and crystal plasticity modeling to predict the evolution of texture, twinning, lattice strains and strength during loading and reloading of beryllium. International Journal of Plasticity, 2022, 150, 103217.	8.8	19
50	Texture evolution during strain-induced martensitic phase transformation in 304L stainless steel at a cryogenic temperature. Metallurgical and Materials Transactions A: Physical Metallurgy and Materials Science, 2006, 37, 3469-3475.	2.2	18
51	Thermal residual strains in depleted α-U. Scripta Materialia, 2013, 69, 566-569.	5.2	18
52	Elastic properties of rolled uranium–10wt.% molybdenum nuclear fuel foils. Scripta Materialia, 2013, 69, 666-669.	5.2	16
53	Crystallographic changes in lead zirconate titanate due to neutron irradiation. AIP Advances, 2014, 4, .	1.3	16
54	Neutron diffraction measurement of residual stresses, dislocation density and texture in Zr-bonded U-10Mo "mini―fuel foils and plates. Journal of Nuclear Materials, 2016, 482, 63-74.	2.7	16

#	Article	IF	CITATIONS
55	The influence of impurities on the crystal structure and mechanical properties of additive manufactured U–14 at.% Nb. Scripta Materialia, 2017, 130, 59-63.	5.2	16
56	In Situ Neutron Diffraction Measurements During Annealing of Deformed Beryllium With Differing Initial Textures. Metallurgical and Materials Transactions A: Physical Metallurgy and Materials Science, 2013, 44, 5665-5675.	2.2	15
57	Neutron Diffraction Measurements and Micromechanical Modelling of Temperatureâ€Dependent Variations in TATB Lattice Parameters. Propellants, Explosives, Pyrotechnics, 2016, 41, 514-525.	1.6	15
58	In situ neutron diffraction studies on the elevated-temperature deformation behavior of a TiAl–W alloy. Applied Physics Letters, 2004, 85, 4654-4656.	3.3	13
59	Using Neutron Diffraction to Investigate Texture Evolution During Consolidation of Deuterated Triaminotrinitrobenzene (d-TATB) Explosive Powder. Crystals, 2017, 7, 138.	2.2	13
60	Measurement and Simulation of Residual Strain in a Laser Welded Titanium Ring. Welding in the World, Le Soudage Dans Le Monde, 2012, 56, 2-8.	2.5	12
61	Incrementally objective implicit integration of hypoelastic–viscoplastic constitutive equations based on the mechanical threshold strength model. Computational Mechanics, 2014, 53, 941-955.	4.0	12
62	lsothermal annealing of shocked zirconium: Stability of the two-phase α/ω microstructure. Acta Materialia, 2015, 91, 101-111.	7.9	12
63	In Situ Time-Resolved Phase Evolution and Phase Transformations in U-6ÂWtÂPct Nb. Metallurgical and Materials Transactions A: Physical Metallurgy and Materials Science, 2019, 50, 2619-2628.	2.2	12
64	Neutron diffraction measurement of residual stresses in Al-clad U–10Mo fuel plates. Journal of Nuclear Materials, 2016, 474, 8-18.	2.7	11
65	Strain-induced phase transformation in a cobalt-based superalloy during different loading modes. Materials Science & Engineering A: Structural Materials: Properties, Microstructure and Processing, 2011, 528, 6051-6058.	5.6	10
66	High energy X-ray diffraction measurement of residual stresses in a monolithic aluminum clad uranium–10wt% molybdenum fuel plate assembly. Journal of Nuclear Materials, 2013, 441, 252-261.	2.7	10
67	In situ neutron diffraction study on temperature dependent deformation mechanisms of ultrafine grained austenitic Fe–14Cr–16Ni alloy. International Journal of Plasticity, 2014, 53, 125-134.	8.8	10
68	A Neutron Diffraction Study of Residual Stress and Plastic Strain in Welded Beryllium Rings. Materials Science Forum, 2002, 404-407, 741-746.	0.3	9
69	High pressure deformation study of zirconium. Powder Diffraction, 2007, 22, 113-117.	0.2	9
70	High energy X-ray diffraction study of the relationship between the macroscopic mechanical properties and microstructure of irradiated HT-9 steel. Journal of Nuclear Materials, 2016, 475, 46-56.	2.7	9
71	Equation of state, phase stability, and phase transformations of uranium-6 wt. % niobium under high pressure and temperature. Journal of Applied Physics, 2018, 123, .	2.5	9
72	Residual stress analysis of in situ surface layer heating effects on laser powder bed fusion of 316L stainless steel. Additive Manufacturing, 2021, 47, 102252.	3.0	8

#	Article	IF	CITATIONS
73	Complementary Measurements of Residual Stresses Before and After Base Plate Removal in an Intricate Additively-Manufactured Stainless-Steel Valve Housing. Additive Manufacturing, 2020, 36, 101555.	3.0	7
74	The influence of peak shock stress on the high pressure phase transformation in zirconium. EPJ Web of Conferences, 2012, 26, 02013.	0.3	5
75	In situ neutron diffraction and Elastic–Plastic Self-Consistent polycrystal modeling of HT-9. Journal of Nuclear Materials, 2012, 425, 228-232.	2.7	5
76	Experimental determination of precision, resolution, accuracy and trueness of time-of-flight neutron diffraction strain measurements. Journal of Applied Crystallography, 2020, 53, 494-511.	4.5	5
77	The Shear Response of Beryllium as a Function of Temperature and Strain Rate. EPJ Web of Conferences, 2018, 183, 02017.	0.3	2
78	The nature of the metamagnetic transition in Heusler alloy Ni44.9Mn43In12.1 studied for magnetic refrigeration application. Materials Science and Engineering B: Solid-State Materials for Advanced Technology, 2022, 283, 115796.	3.5	2
79	Evolution of Texture and Deformation Mechanisms During Repeated Deformation and Heat Treating Cycles of U-6Nb. Metallurgical and Materials Transactions A: Physical Metallurgy and Materials Science, 2021, 52, 2195-2207.	2.2	1
80	Probing Mesoscopic Strain Evolution during Creep Deformation: An In-Situ Neutron Diffraction Study. Materials Research Society Symposia Proceedings, 2004, 840, Q7.5.1.	0.1	0
81	Data-driven analysis of neutron diffraction line profiles: application to plastically deformed Ta. Scientific Reports, 2022, 12, 5628.	3.3	0